PENG TIAN
LEI NIE
and
GAOFENG ZHAN

# Specific surface area of construction minerals

*Pore characteristics are the key index to characterize the surface characteristics of mineral materials. The surface pore characteristics of road of construction minerals are the key indexes to influence the adhesion and pavement performance of asphalt mixture. Adsorption and desorption experiments on limestone, andesite and basalt. Using nitrogen as adsorbent in the experiment. Through the calculation, the specific surface area and pore size distribution of multiple groups of mineral materials were obtained. The results show that the pore characteristics of the mineral surface are closely related to the composition and genesis. The average pore size and specific surface area of limestone are much higher than basalt and andesite. The average pore diameter of limestone is 5.6 times than that of basalt and 8 times than that of andesite. The BET specific surface area is 4.5 times than that of basalt and 7.8 times than that of andesite. Limestone is a sedimentary rock, the surface is rougher than that of basalt and andesite. There is a great difference in the texture of limestone from different quarries. The average pore size of basalt and andesite is similar, and the surface pore characteristics of them even produced by different quarries are close.*

***Keywords:*** *Specific surface area, pore, composition, adsorption, characteristic model.*

## 1. Introduction

At a constant temperature, a certain amount of gas adsorption can be found on the solid surface, corresponding to the pressure of the adsorbed mass. The adsorption isotherm can be obtained by determining the corresponding adsorption quantity under a series of relative pressure [1]. Adsorption isotherms are the basic data on the adsorption phenomenon and the surface and pores of the solid. From the study of the surface and pore properties of the mineral, the specific surface area and pore size distribution can be calculated.

Adsorption isothermal curve is widely used in many industries [2-4]. In geological science, it can be used in surface fractal research based on adsorption isotherm and its application in earth science. It can be analyzed that the adsorption of $CH_4$ and $CO_2$ in mixed gas by coal shows different adsorption characteristics [5-6].

The surface structure of building mineral materials is complex, and the pore characteristics have a far-reaching impact on the characteristics of the building mixture. Based on the mineral surface characteristics, can play and optimize the role of mineral materials in the construction. A total of three types of stone material for adsorption and desorption experiments. Three types of experimental materials for the limestone, andesite and basalt. Three samples of three different quarries were prepared for each type of material for a total of nine experimental samples.

By comparing the characteristics of surface pore size and surface area of mineral material, we can see that the pore diameter is proportional to the change of specific surface area [7-9]. Based on the comprehensive analysis of surface porosity characteristics and mineral composition and genesis, it is found that the pore characteristics of mineral surface are closely related to the composition and genesis of the mineral aggregate.

## 2. Preparations

### 2.1 Specimens

There are three types of samples for the experiment, from nine quarries. The key to the adsorption experiment is that the adsorbed gas molecules are effectively adsorbed on the surface of the measured solid and filled in the pores. The gravel for road construction is large in size. Before the experiment, the specimens must be crushed and treated as a particle with a diameter of 2-4 mm as shown in Fig.1.

Because the purpose of the experiment is to determine the specific surface area and pore size of the coarse aggregate, so the specimens should not be ground to powder, that will be losing the porosity characteristics of the mineral aggregate surface [10-11].

After the samples were crushed to qualified size, the specimens were heated to 120°C under atmospheric pressure to remove the water molecules adsorbed on the surface.

Messrs. Peng Tian, Lei Nie and Gaofeng Zhan, College of Construction Engineering, Jilin University, Changchun 130 026 and Peng Tian and Gaofeng Zhan, Jilin Jianzhu University, Changchun 130 118, China. Email: nielei@jlu.edu.cn

Fig.1 Specimens

### 2.2 Composition

The basalt is an extrusive magmatic rock with a $SiO_2$ content of 45-52%. The main minerals are stone and plagioclase, with a few quartz, alkali-feldspar and olivine. The andesite is an intrusive magmatic rock with a $SiO_2$ content of 53.5-62%. The main minerals are neutral-plagioclase and hornblende, plus some biotite. The limestone is carbonate rock with calcite as the main component, sometimes contains dolomite, clay minerals and clastic minerals [12-13]. The main components of crushed stone is shown in Table 1.

### 3.2 Instrument

F-Sorb 3400 specific surface area and pore size analysis instrument was used to study the adsorption and desorption of specimens. This device is suitable for the materials which containing a large number of mesoporous and microporous. It can measure the specific surface area of 0.01m$^2$/g or more

The measuring aperture range of the device is between 2-200nm. The relative error is less than 2%.High-purity nitrogen (99.99%) is used as the carrier gas and adsorbate gas.

When the relative pressure is lower than 0.05, the number of nitrogen molecules required for layer adsorption cannot be reached, and it is difficult to form a nitrogen molecule adsorption equilibrium. When the relative pressure is higher than 0.35, the phenomenon of capillary condensation will occur, affecting the physical adsorption layer, the adsorption layer no longer increases [14-15]. Therefore, the experimental relative pressure is controlled between 0.05 and 0.35.

Table 1: Original images and processed images

| No. | Crystalline mineral | Phenocryst | Calcite | Agglutinate material |
|---|---|---|---|---|
| Basalt-01 | 50-70% | 4-8% | - | - |
| Basalt-02 | 60-80% | 5-9% | - | - |
| Basalt-03 | 70-80% | 3-7% | - | - |
| Andesite-01 | - | 15-20% | - | - |
| Andesite-02 | - | 5-8% | - | - |
| Andesite-03 | - | 8-10% | - | - |
| Limestone-01 | - | - | 0.90 | 0.05 |
| Limestone-02 | - | - | 0.80 | 0.05 |
| Limestone-03 | - | - | 0.87 | 0.07 |

### 3.3 Adsorption and desorption experiment

The specimens were placed in the glass container and heated for 2 hours under the vacuum 150$^o$ for pretreatment. Then the specimens were placed on F-sorb 3400, ventilate for 3 minutes and heat for 30 minutes, as shown in Fig.2.

## 3. Adsorption and desorption experiments

### 3.1 Equipment and settings

The pore size is divided into three types: the pore size r>50nm is the big pore, the pore diameter r<2nm is the micro-pore. Between the two is called the middle hole.

Fig.2 Specimens in the glass container

The liquid nitrogen was injected into the experimental container, and the distance between the liquid level and the cup mouth was about 2 cm.

In a state of constant temperature and pressure balance, the amount of gas adsorbed on the gravel surface is maintained at a certain value [16]. When the pressure changes, the amount of adsorption on the surface of the crushed stone is also changed, and the new balance will be reached. Nitrogen adsorption and desorption experiments are carried out on the specimens of limestone, andesite and basalt respectively. Each type of sample has three groups from three different quarries. There are nine groups of samples for the experiment.

## 4. Aperture and specific surface area analysis

### 4.1 Pore size

The surface of road construction minerals is rough and the structure is complex with many pore sizes coexist. At a certain temperature, the vapor condenses into liquid in the pores and porous medium structure, which is called capillary condensation phenomenon [17]. According to the capillary condensation theory, the pore radius of capillary condensation increases with the increase of $P/P_0$ value. There is a $R_k$ value of critical void radius corresponding to

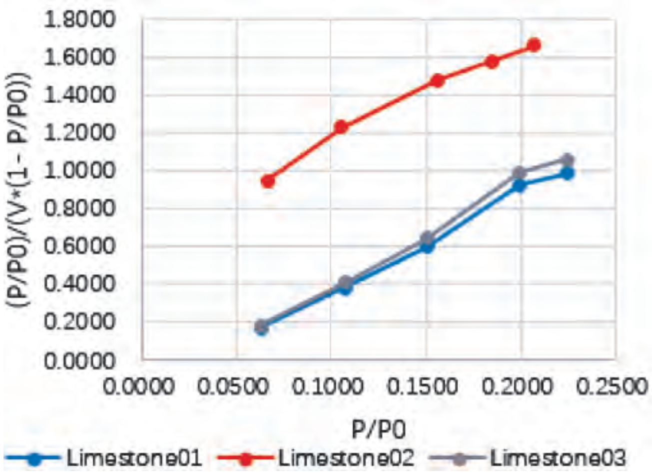


Fig.3 BET curve of limestone

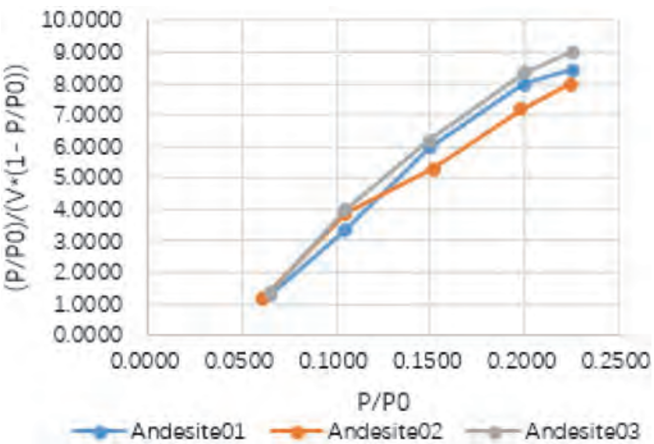


Fig.4 BET curve of andesite

### 4.2 Specific area

I. Langmuir proposed the monolayer adsorption theory in 1916, and its expression equation is the Langmuir isothermal equation.

The basic assumption is: (1) adsorbent surface uniformity; (2) there is no interaction between adsorbed molecules, and the heat of adsorption has nothing to do with the coverage rate; (3) adsorption monolayer adsorption. The expression equation is shown in formula (2):

$$\frac{V}{V_m} = \theta = \frac{BP}{1+BP} \quad \ldots \quad (2)$$

where $V$ represents the amount of adsorbed gas, $V_m$ is the saturated adsorption capacity of the monolayer, $\theta$ is the surface coverage, $P$ is the adsorption pressure, $B$ is the adsorption constant.

S. Brunauer, P. Emmett, and E. Teller proposed the BET multi-layer adsorption theory in 1938, the expression equation of which is the BET equation [18-19].

The basic assumption is that: (1) solid surface uniformity, physical adsorption is carried out in a multi-layer manner, (2) except the first layer of adsorption heat of the remaining layers of the adsorption heat is equal to the adsorption of the liquid heat, there is no time line between layer and layer, continuous adsorption [20], [21]. The expression equation is shown in formula (3):

$$\frac{P/P_0}{V(1-P/P_0)} = \frac{C-1}{V_m C} \times P/P_0 + \frac{1}{V_m C} \quad \ldots \quad (3)$$

where $V$ is the amount of gas adsorption, $V_m$ is the saturated adsorption capacity of the monolayer, $P$ is the adsorption pressure, $P_0$ is the saturated vapor pressure of the adsorbate, the $P/P_0$ value. At this point, the holes with a radius of less than $R_k$ are filled with liquid nitrogen. The relationship between pore $R_k$ of capillary condensate and pressure of adsorbed mass can be expressed by formula (1):

$$R_k = \frac{-0.414}{\log\left(\frac{P}{P_0}\right)} \quad \ldots (1)$$

The $R_k$ value of critical void radius is directly related to the relative pressure $P/P_0$. The formula is also effective for the desorption process of adsorbent. When $P/P_0$ is lower than a certain value, the condensate in the pore whose void radius is larger than $R_k$) is gasified and desorbed.

Table 2: Data of adsorption and desorption for limestone

| No. | $P/P_0$ | Adsorption quantity of unit | $(P/P_0)/(V*(1- P/P_0))$ | BET specific surface area |
|---|---|---|---|---|
| Limestone 01 | 0.2241 | 0.2916 | 0.9909 | 0.9845 |
| Limestone 01 | 0.1997 | 0.2682 | 0.9304 | 0.9340 |
| Limestone 01 | 0.1500 | 0.2924 | 0.6036 | 1.0817 |
| Limestone 01 | 0.1072 | 0.3136 | 0.3830 | 1.2186 |
| Limestone 01 | 0.0628 | 0.3911 | 0.1713 | 1.5954 |
| Limestone 02 | 0.2070 | 0.1563 | 1.6695 | 0.5395 |
| Limestone 02 | 0.1848 | 0.1431 | 1.5844 | 0.5077 |
| Limestone 02 | 0.1565 | 0.1251 | 1.4836 | 0.4592 |
| Limestone 02 | 0.1056 | 0.0957 | 1.2332 | 0.3726 |
| Limestone 02 | 0.0661 | 0.0745 | 0.9499 | 0.3030 |
| Limestone 03 | 0.2241 | 0.3120 | 1.0602 | 1.0534 |
| Limestone 03 | 0.1997 | 0.2869 | 0.9955 | 0.9994 |
| Limestone 03 | 0.1500 | 0.3129 | 0.6459 | 1.1574 |
| Limestone 03 | 0.1072 | 0.3356 | 0.4098 | 1.3039 |
| Limestone 03 | 0.0628 | 0.4185 | 0.1833 | 1.7071 |

Table 3: Data of adsorption and desorption for andesite

| No. | $P/P_0$ | Adsorption quantity of unit | $(P/P_0)/(V^*(1- P/P_0))$ | BET specific surface area |
|---|---|---|---|---|
| Andesite 01 | 0.2252 | 0.0345 | 8.4228 | 0.1164 |
| Andesite 01 | 0.1998 | 0.0312 | 7.9921 | 0.1088 |
| Andesite 01 | 0.1494 | 0.0295 | 5.9617 | 0.1091 |
| Andesite 01 | 0.1045 | 0.0351 | 3.3278 | 0.1366 |
| Andesite 01 | 0.0648 | 0.0544 | 1.2730 | 0.2214 |
| Andesite 02 | 0.2241 | 0.0362 | 7.9748 | 0.1223 |
| Andesite 02 | 0.1981 | 0.0344 | 7.1868 | 0.1199 |
| Andesite 02 | 0.1514 | 0.0337 | 5.2916 | 0.1245 |
| Andesite 02 | 0.1051 | 0.0303 | 3.8815 | 0.1178 |
| Andesite 02 | 0.0607 | 0.0565 | 1.1429 | 0.2311 |
| Andesite 03 | 0.2252 | 0.0389 | 9.0187 | 0.1313 |
| Andesite 03 | 0.1998 | 0.0361 | 8.3484 | 0.1258 |
| Andesite 03 | 0.1494 | 0.0347 | 6.1893 | 0.1285 |
| Andesite 03 | 0.1045 | 0.0359 | 3.9651 | 0.1399 |
| Andesite 03 | 0.0648 | 0.0610 | 1.3287 | 0.2489 |

Table 4: Data of adsorption and desorption for basalt

| No. | $P/P_0$ | Adsorption quantity of unit | $(P/P_0)/(V^*(1- P/P_0))$ | BET specific surface area |
|---|---|---|---|---|
| Basalt 01 | 0.2270 | 0.0498 | 5.9014 | 0.1674 |
| Basalt 01 | 0.2002 | 0.0612 | 4.0906 | 0.2130 |
| Basalt 01 | 0.1484 | 0.0553 | 3.1544 | 0.2048 |
| Basalt 01 | 0.1033 | 0.0585 | 1.9693 | 0.2283 |
| Basalt 01 | 0.0628 | 0.0527 | 1.2707 | 0.2151 |
| Basalt 02 | 0.2247 | 0.0560 | 5.1757 | 0.1889 |
| Basalt 02 | 0.1992 | 0.0562 | 4.4295 | 0.1957 |
| Basalt 02 | 0.1510 | 0.0533 | 3.3397 | 0.1968 |
| Basalt 02 | 0.1040 | 0.0547 | 2.1211 | 0.2134 |
| Basalt 02 | 0.0648 | 0.0599 | 1.1554 | 0.2439 |
| Basalt 03 | 0.2247 | 0.0648 | 4.4741 | 0.2185 |
| Basalt 03 | 0.1992 | 0.0634 | 3.9242 | 0.2209 |
| Basalt 03 | 0.1510 | 0.0639 | 2.7845 | 0.2360 |
| Basalt 03 | 0.1040 | 0.0605 | 1.9194 | 0.2359 |
| Basalt 03 | 0.0648 | 0.0585 | 1.1829 | 0.2383 |

$P/P_0$ is the relative pressure of the gas, $C$ is the strength dependent constant of gas and solid interaction [22-23] .

First, calculate the monolayer adsorption, and then get the specific surface area of them [24]. Data from $V$ and $P/P_0$ can be measured by experimental equipment. There is direct relationship between $V_m$ and the specific surface area. So, it is necessary to calculate the value of $V_m$. After that, the specific surface area of the aggregate can be calculated. The BET line diagram is shown in Fig.6.

Where the vertical axis is $Y = \frac{P/P_0}{V(1-P/P_0)}$, the horizontal axis is X = $P/P_0$, the slope is $s = \frac{C-1}{V_m C}$, the intercept is $i = \frac{1}{V_m C}$.

As shown in Fig.4, $V_m$ can be calculated by formula (4):

$$V_m = \frac{V(1-P/P_0)((C-1)P/P_0+1)}{CP/P_0} \quad ...(4)$$

When using nitrogen as the adsorbate, the specific surface area $S_g$ can be obtained by the formula (5):

$$S_g = \frac{4.36 \cdot V_m}{W} \quad ... \quad (5)$$

where the unit of $V_m$ is ml, the unit of $W$ is g, and the unit of the surface $S_g$ is $m^2/g$.

### 4.3 Analysis of pore size and specific surface area

Based on the theory of specific surface area analysis and pore size analysis, the data obtained from adsorption experiments are processed. The slope and intercept of specimens are shown in Table 5.

The value of $V_m$, $C$ and linear fitting are shown in Table 6. The value of linear fitting is close to 1, that means the fitting effect is good. The parameters of different types of mineral materials are very obvious.

Based on the formula mentioned above, we can calculate the mean of pore size and specific surface area, as shown in Table 7.

The coordinate system is set up with the number of experiments as horizontal axis and the experimental results as vertical axis. Plot the BET and Langmuir specific surface area curves in this coordinate system as shown in Fig.7.

The calculated specific surface area of Langmuir is larger than that of BET. The curves of BET and Langmuir showed the same trend.

The coordinate system with the average aperture of x-axis and the BET specific surface of Y-axis is established. Draw a scatter plot of nine specimens, as shown in Fig.8.

In the Fig.8, the scatter points are basically linearly distributed. It shows that the specific surface area is proportional to the mean pore size.

The distribution of limestone scattered points is far away from the distribution area of andesite and basalt and located

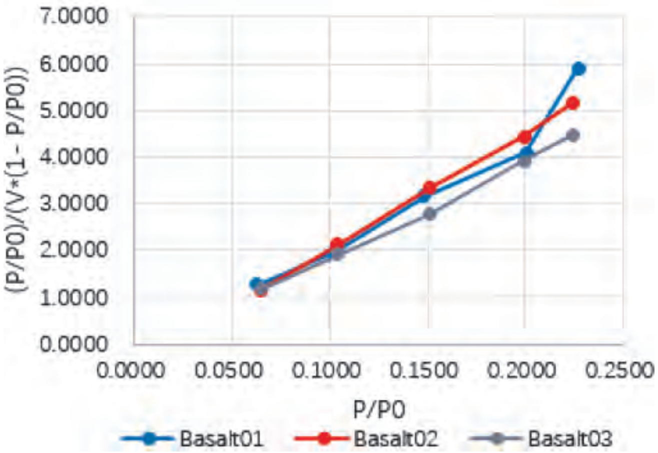


Fig.5 BET curve of basalt

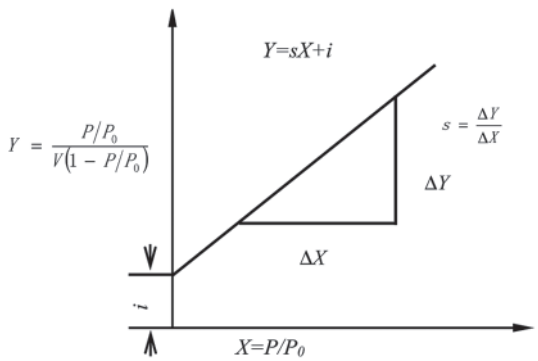


Fig.6 BET line diagram

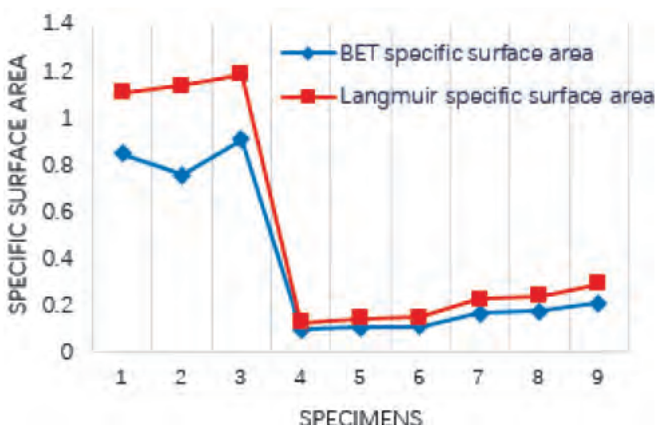


Fig.7 Specific surface area

in the upper right corner. It is indicating that the pore size of limestone and BET are larger than the surface. This is consistent with the origin of limestone. The distribution of scattered points between basalt and andesite is very close, indicating that their pore size and specific surface area are close, and the composition and genesis of andesite and basalt are close to each other.

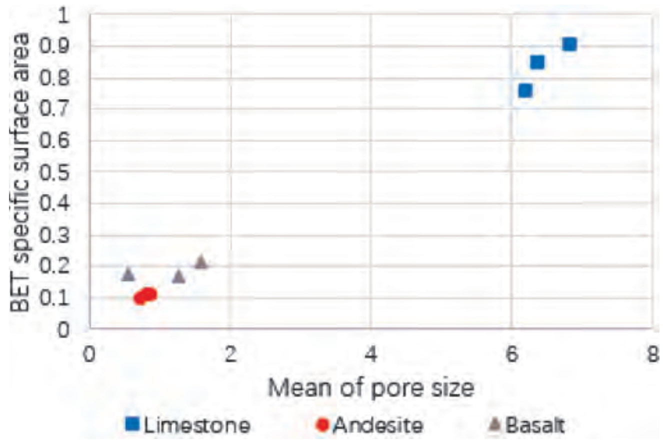


Fig.8 Scatter plot of BET and mean pore size

TABLE 5: BET GEOMETRIC PARAMETERS

| No. | Slope | Intercept |
|---|---|---|
| Limestone 01 | 5.2988 | 0.1725 |
| Limestone 02 | 5.0944 | 0.6571 |
| Limestone 03 | 5.6697 | 0.1846 |
| Andesite 01 | 45.9241 | 1.4343 |
| Andesite 02 | 40.5939 | 0.9074 |
| Andesite 03 | 47.5849 | 1.2880 |
| Basalt 01 | 26.2919 | 0.6233 |
| Basalt 02 | 24.8895 | 0.4579 |
| Basalt 03 | 20.6675 | 0.2171 |

TABLE 6: LINEAR FITTING RESULTS OF THE EXPERIMENT

| No | $V_m$ | C | Linear fitting |
|---|---|---|---|
| Limestone 01 | 0.1951 | 29.71 | 0.9967 |
| Limestone 02 | 0.1739 | 8.75 | 0.9891 |
| Limestone 03 | 0.2087 | 29.71 | 0.9967 |
| Andesite 01 | 0.0225 | 31.02 | 0.9912 |
| Andesite 02 | 0.0252 | 43.73 | 0.9916 |
| Andesite 03 | 0.0262 | 37.38 | 0.9914 |
| Basalt 01 | 0.0390 | 41.18 | 0.9733 |
| Basalt 02 | 0.0409 | 53.36 | 0.9996 |
| Basalt 03 | 0.0489 | 94.21 | 0.9986 |

TABLE 7: THE MEAN OF PORE SIZE AND SPECIFIC SURFACE AREA

| No | Specimens | Mean of pore size | BET specific surface area | Langmuir specific surface area |
|---|---|---|---|---|
| 1 | Limestone 01 | 6.3672 | 0.849 | 1.1053 |
| 2 | Limestone 02 | 6.1893 | 0.7568 | 1.1382 |
| 3 | Limestone 03 | 6.8129 | 0.9084 | 1.1827 |
| 4 | Andesite 01 | 0.7337 | 0.0978 | 0.1273 |
| 5 | Andesite 02 | 0.8224 | 0.1097 | 0.1447 |
| 6 | Andesite 03 | 0.8559 | 0.1141 | 0.1496 |
| 7 | Basalt 01 | 1.2716 | 0.1695 | 0.2284 |
| 8 | Basalt 02 | 0.5625 | 0.1781 | 0.2404 |
| 9 | Basalt 03 | 1.5961 | 0.2128 | 0.2934 |

## 5. Conclusions

Limestone, andesite and basalt are used as experimental materials for adsorption and desorption experiments. Based on the theory of specific surface area and pore size, the specific surface area and pore size distribution of nine groups are obtained. The results show that the pore characteristics of the mineral surface are closely related to the composition and genesis. The mean pore size of limestone is 6.46nm. It is 5.6 times that of basalt and 8 times that of andesite. The BET specific surface area of limestone is $0.84m^2/g$, it is 4.5 times that of basalt and 7.8 times that of andesite. Limestone is a sedimentary rock, the surface is rougher than that of basalt and andesite.

There is a great difference in the characteristics of limestone from different quarries. The mean pore size of basalt and andesite are similar, and the surface pore characteristics of them even produced from different quarries are close.


## Acknowledgment

This study was supported by the 13th Five-Year Science of the Education Department in Jilin Province, Jilin Education Science Planning Project (GH150340) and technology research project planning 2017 in Jilin provincial industrial innovation special fund project (2017C030-3).


## References


1. Inagaki, M. (2016): "Chapter 11: Gas Adsorption/ Desorption Isotherm for Pore Structure Characterization" in Materials Science and Engineering of Carbon, Kidlington, Oxford OX5 1 GB, UK, Elsevier Inc, 2016, pp. 227-247.
2. Hu, S. (2016): "Effects of gas adsorption on mechanical properties and erosion mechanism of coal." *J. Nat Gas Sci Eng*, vol. 30, pp. 531-538, 2016.
3. Tian, P.: "Characteristics' relation model of asphalt pavement performance based on factor analysis," *Int J. Pavement Res & Technol.* to be published.
4. Ganesan, A. (2016): "Activated graphene-derived porous carbon with exceptional gas adsorption properties." *Micropor Mesopor Mat*, vol. 220, no. 15, pp. 21-27, 2016.
5. Rouquerol, J. (2016): "Surface excess amounts in high-pressure gas adsorption: Issues and benefits." *Colloids Surf. A*, vol. 496, no. 5, pp. 3-12, 2016.
6. Zhao, J. L. (2016): "Pore-scale simulation of shale gas production considering the adsorption effect," *Int. J. Heat Mass Transfer*, vol. 103, pp. 1098-1107, 2016.
7. Li, T. F. (2016): "Application of low pressure gas adsorption to the characterization of pore size distribution of shales: An example from Southeastern Chongqing area, China," *J. Nat. Gas Geo*, vol. 1, no. 3, pp. 221-230, 2016.
8. Fredrich, J. T. (1995): "Imaging the pore structure of geomaterials," *SCI*, vol. 268, no. 5208, pp.276-279, 1995.
9. Nimmo, J. (2004): "Porosity and pore size distribution," *Encycl. Soils Environ*, vol. 3, pp. 295-303, 2004.
10. Han, H. (2016): "Influence of particle size on gas-adsorption experiments of shales: An example from a Longmaxi Shale sample from the Sichuan Basin, China," *Fuel*, vol. 186, pp. 750-757, 2016.
11. Matellato, S. (2016): "Impact of sample preparation on the specific surface area of synthetic ettringite," *Cem. Concr. Res*, vol. 86, pp.20-28, 2016.
12. Tian, P.: "Chemical Composition Influence on Macadam Surface Texture," *Chem. Eng. Trans*, to be published.
13. Zaffar, M. (2015): "Pore Size Distribution of Clayey Soils and Its Correlation with Soil Organic Matter," *Pedosphere*, vol. 25, no. 2, pp. 240-249, 2015.
14. Liu, X. F. (2016): "Fractal characteristics of coal samples utilizing image analysis and gas adsorption," *Fuel*, vol. 182, pp. 314-322, 2016.
15. Saidian, M. (2016): "Effect of clay and organic matter on nitrogen adsorption specific surface area and cation exchange capacity in shales (mudrocks)," *J. Nat. Gas Sci. Eng*, vol. 33, pp.1095-1106, 2016.
16. Dubinin, M. M. (1989): "Fundamentals of the theory of adsorption in micropores of carbon adsorbents: characteristics of their adsorption properties and microporous structures." *Carbon*, vol. 27, no. 3, pp. 457-467, 1989.
17. Rouquerol, J. (2007): "Is the BET equation applicable to microporous adsorbents?" *Stud. Surf. Sci. Catal*, vol. 160, pp. 49-56, 2007.
18. Heister, K. (2016): "How accessible is the specific surface area of minerals? A comparative study with Al-containing minerals as model substances," *Geoderma*, vol. 263, pp. 8-15, 2016.
19. Lapham, D. P. (2017): "Gas adsorption on commercial magnesium stearate: Effects of degassing conditions on nitrogen BET surface area and isotherm characteristics," *Int. J. Pharm*, vol.530, no. 1-2, pp. 364-376, 2017.
20. Re, G. Lo (2015): "A facile method to determine pore size distribution in porous scaffold by using image processing," *Micron*, vol. 76, pp. 37-45, 2015.
21. Zeng, Q. (2015): "Discussion of 'Numerical simulation of moisture transport in concrete based on a pore size distribution model,'" *Cem. Concr. Res*, vol. 73, pp. 63-66, 2015.
22. Madani, S. H. (2015): "Uncertainty in pore size distribution derived from adsorption isotherms: I. Classical methods," *Microporous Mesoporous Mater*, vol. 214, pp. 210-216, 2015.
23. Madani, S. H. (2015): "Uncertainty in pore size distribution derived from adsorption isotherms: II. Adsorption integral approach." *Microporous Mesoporous Mater*, vol. 214, pp. 217-223, 2015.
24. Akhondi, E. (2015): "Improved design and protocol for evapoporometry determination of the pore-size distribution," *J. Membr. Sci*, vol. 496, pp. 334-343, 2015.